Bioorganic & Medicinal Chemistry 18 (2010) 2678–2685

Contents lists available at ScienceDirect

Bioorganic & Medicinal Chemistry

journal homepage: www.elsevier.com/locate/bmc

Zinc(II) complexes of the second-generation quinolone antibacterial drug enrofloxacin: Structure and DNA or albumin interaction

Alketa Tarushi [a], Catherine P. Raptopoulou [b], Vassilis Psycharis [b], Aris Terzis [b], George Psomas [a], Dimitris P. Kessissoglou [a,*]

[a] Department of General and Inorganic Chemistry, Faculty of Chemistry, Aristotle University of Thessaloniki, PO Box 135, GR-54124 Thessaloniki, Greece
[b] Institute of Materials Science, NCSR 'Demokritos', GR-15310 Aghia Paraskevi Attikis, Greece

ARTICLE INFO

Article history:
Received 29 December 2009
Revised 10 February 2010
Accepted 12 February 2010
Available online 18 February 2010

Keywords:
Zinc complexes
Enrofloxacin
Interaction with calf-thymus DNA
Interaction with serum albumins

ABSTRACT

Zinc mononuclear complexes with the second-generation quinolone antibacterial drug enrofloxacin in the absence or presence of a nitrogen donor heterocyclic ligand 1,10-phenanthroline or 2,2′-bipyridine have been synthesized and characterized. Enrofloxacin is on deprotonated mode acting as a bidentate ligand coordinated to zinc ion through the ketone and a carboxylato oxygen atoms. The crystal structure of bis(enrofloxacinato)(1,10-phenanthroline)zinc(II), **2**, has been determined by X-ray crystallography. The biological activity of the complexes has been evaluated by examining their ability to bind to calf-thymus DNA (CT DNA) with UV and fluorescence spectroscopies. UV studies of the interaction of the complexes with DNA have shown that they can bind to CT DNA and the DNA binding constants have been calculated. Competitive studies with ethidium bromide (EB) have shown that the complexes exhibit the ability to displace the DNA-bound EB indicating that they bind to DNA in strong competition with EB for the intercalative binding site. The complexes exhibit good binding propensity to human and bovine serum albumin proteins having relatively high binding constant values.

1. Introduction

Zinc has an important role in various biological systems,[1] since it is critical for numerous cell processes and is a major regulatory ion in the metabolism of cells.[2] In the literature, diverse zinc complexes with biological activity are reported. More specifically, crystal structures of zinc complexes with drugs used for the treatment of Alzheimer disease[3] or presenting anticonvulsant,[4] antidiabetic,[5] anti-inflammatory,[6] antimicrobial,[7] antiproliferative and/or antitumor[8–10] and bactericidal[11] activity are now available.

Enrofloxacin (=Herx, Fig. 1), a typical second-generation quinolone antimicrobial drug[12] with a broad spectrum of activity against a wide range of Gram-negative and Gram-positive bacteria, including those resistant to β-lactam antibiotics and sulfonamides,[13] is the first fluoroquinolone developed for veterinary application and is potentially available for the treatment of some urinary tract, respiratory tract and skin infectious diseases in pets and livestock.[14] Quinolones (quinolonecarboxylic acids or 4-quinolones) are commonly used as treatment for many infections[12] since they can act as antibacterial drugs that effectively inhibit DNA replication. Enrofloxacin is also used for the treatment of urinary tract infections, pyelonephritis, sexually transmitted diseases, prostatitis, skin and tissue infections, urethral and cervical gonococcal infections.[15,16] A thorough survey of the literature has revealed that only a Zn(II)[17] and three Cu(II) enrofloxacin complexes[18,19] have been structurally characterized.

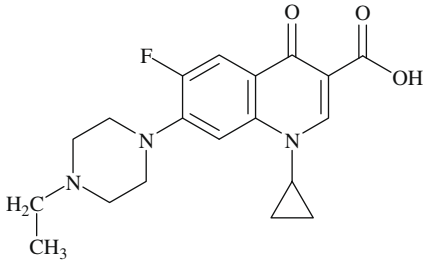

Figure 1. Enrofloxacin (Herx = 1-cyclopropyl-7-(4-ethyl-piperazin-1-yl)-6-fluoro-4-oxo-1,4-dihydro-quinoline-3-carboxylic acid).

We have initiated the study of zinc(II) complexes with quinolone antimicrobial agents.[17,20] In this context, the synthesis, the characterization and the DNA or albumin binding properties of the novel neutral mononuclear zinc complexes with enrofloxacin in the absence or presence of the N,N′-donor heterocyclic ligands 1,10-phenanthroline (=phen) or 2,2′-bipyridine (=bipy) are presented. The crystal structure of $[Zn(erx)_2(phen)]\cdot 4MeOH$, **2**·4MeOH, has been determined by X-ray crystallography. The ability of the complexes

* Corresponding author. Tel.: +30 2310997723; fax: +30 2310997738.
E-mail address: kessisog@chem.auth.gr (D.P. Kessissoglou).

0968-0896/$ - see front matter © 2010 Elsevier Ltd. All rights reserved.
doi:10.1016/j.bmc.2010.02.021

to bind to CT (calf-thymus) DNA has been investigated by UV spectroscopic titration and their intrinsic binding constants, K_b, with CT DNA have been determined. Competitive binding titration with ethidium bromide (EB), one of the most widely used intercalative agents and fluorescence probes for DNA structure, have been employed in the study of the interaction of the complexes with CT DNA in order to investigate a potential intercalative binding mode. The affinity of Herx and its complexes for human (HSA) and bovine (BSA) serum albumin, proteins responsible for the transport of drugs in the body, has been investigated by fluorescence spectroscopy.

2. Results and discussion

2.1. Synthesis and spectroscopic study of the complexes

The synthesis of complexes was achieved via the reaction of enrofloxacin, deprotonated with KOH, in the absence (Eq. 1 for **1**) or presence of a N-donor ligand for example, 1,10-phenanthroline (Eq. 2) for **2**, with $ZnCl_2$ under air, according to the equations:

$$ZnCl_2 + 2C_{18}H_{21}FN_3O{-}COOH + 2KOH \rightarrow [Zn(C_{18}H_{21}FN_3O{-}COO)_2(H_2O)_2] + 2KCl \quad (1)$$

$$ZnCl_2 + 2C_{18}H_{21}FN_3O{-}COOH + 2KOH + C_{12}H_8N_2 \rightarrow [Zn(C_{18}H_{21}FN_3O{-}COO)_2(C_{12}H_8N_2)] + 2KCl + 2H_2O \quad (2)$$

In the IR spectra of the complexes, the observed absorption bands at 3442(br,m) cm^{-1}, 1736(s) cm^{-1} and 1254(s) cm^{-1} attributed to the stretching vibrations ν(H–O), $\nu(C{=}O)_{carboxyl}$, $\nu(C{-}O)_{carboxyl}$, respectively, of the carboxylic group (–COOH) of the Herx molecule, have been replaced by two very strong characteristic bands in the range of 1580–1615 cm^{-1} and 1375–1380 cm^{-1} assigned as antisymmetric, $\nu_{asym}(C{=}O)$, and symmetric, $\nu_{sym}(C{=}O)$, stretching vibrations, respectively. The difference Δ [$=\nu_{asym}(C{=}O) - \nu_{sym}(C{=}O)$], a useful characteristic tool for determining the coordination mode of the carboxylato ligands, gives a Δ value falling in the range 200–240 cm^{-1} indicating a monodentate coordination mode.[21] The vibration $\nu(C{=}O)_{ketone}$ is slightly shifted from 1627 cm^{-1} up to 1638 cm^{-1} upon bonding. The overall changes of the IR spectra suggest that enrofloxacinato ligand is coordinated to the metal via the ketone oxygen and a carboxylate oxygen.[17,18]

2.2. Crystal structure of [Zn(erx)$_2$(phen)]·4MeOH, 2·4MeOH

A drawing of the molecular structure of **2** (Fig. 2) and selected bond distances and angles are listed in Table 1.

The complex is mononuclear and the enrofloxacinato ligands behave as deprotonated bidentate ligands coordinated to zinc ion via the ketone oxygen and a carboxylate oxygen. There are four methanol solvate molecules. The quinolone ligands in the structurally characterized zinc–quinolone complexes reported so far, act as either neutral[22,23] or deprotonated[11,23–25] bidentate ligands coordinated through the ketone oxygen and a carboxylato oxygen atom, as protonated counter cations,[26] and as deprotonated tridentate ligands bound to zinc through the ketone oxygen, a carboxylate oxygen and the piperazine nitrogen atom.[22]

In **2**, the zinc atom is in a distorted octahedral environment formed by two nitrogen atoms from the 1,10-phenanthroline ligand and four oxygen atoms from two enrofloxacinato ligands. The arrangement of two enrofloxacinato ligands is such that the two ketone oxygen atoms [O(3)–Zn(1)–O(3)′ = 93.7(2)°] are in a *cis* and the two carboxylato oxygen atoms [O(1)–Zn(1)–O(1)′ = 172.1(2)°] are in a *trans* arrangement. On the contrary, in the crystal structure of [Zn(oxolinato)$_2$(phen)],[20] a Zn(II)–quinolone complex that we have previously reported, the two carboxylato oxygen atoms are in a *cis* arrangement. The Zn–O_{carb} distances of oxygen atoms in *trans* position [Zn(1)–O(1) = 2.060(3) Å] are shorter than the Zn–O_{ket} ones [Zn(1)–O(3) = 2.121(3) Å] occupying *cis* positions. The N(11)–Zn(1)–N(11)′ angle of 77.4(2)° is similar to reported values of other chelating polycyclic diimines.[20,27,28] The 1,10-phenanthroline ligand is planar with the zinc atom lying in this plane.

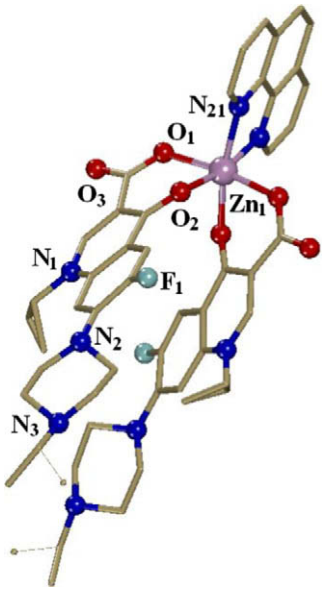

Figure 2. A drawing of the molecular structure of **2** with only the heteroatoms labeling.

Table 1
Selected bond distances and angles for complex **2**

Bond (Å)			
Zn(1)–N(1)	2.155(3)	C(1)–O(1)	1.256(5)
Zn(1)–O(1)	2.060(3)	C(1)–O(2)	1.248(6)
Zn(1)–O(3)	2.121(3)	C(3)–O(3)	1.262(5)
Angles (°)			
N(11)–Zn(1)–O(1)	88.4(1)	O(1)–Zn(1)–O(3)	84.8(1)
N(11)–Zn(1)–O(3)	169.0(1)	O(1)–Zn(1)–O(1)'	172.1(2)
N(11)–Zn(1)–N(11)'	77.4(2)	O(1)′–Zn(1)–O(3)	89.8(1)
N(11)′–Zn(1)–O(3)	94.9(1)	O(3)–Zn(1)–O(3)′	93.7(2)
N(11)′–Zn(1)–O(1)	97.8(1)		

Due to the poor quality of the crystals of [Zn(erx)$_2$(bipy)], **3,** the X-ray diffraction data are not discussed in details but only the geometrical characteristics and the bond connectivities are given. From this experiment the isostructural nature of **2** and **3** was confirmed. The complex is mononuclear with the enrofloxacinato ligands behaving as deprotonated bidentate ligands bound to zinc ion via the ketone oxygen and a carboxylato oxygen (Fig. 3). The zinc atom is in a distorted octahedral environment formed by two nitrogen atoms from the 2,2′-bipyridine ligand and four oxygen atoms from two enrofloxacinato ligands. The two carboxylato oxygen atoms are in *trans* and the two ketone oxygen atoms are in *cis* arrangement.

The complex [Zn(erx)$_2$(H_2O)$_2$], **1** is mononuclear with the enrofloxacinato ligands behaving as deprotonated bidentate ligands bound to zinc ion via the ketone oxygen and a carboxylato oxygen. The zinc atom is expected to be in a distorted octahedral environment formed by six oxygen atoms provided by two water and two enrofloxacinato ligands. Concerning the position of two water molecules in the octahedron we suggest *trans* arrangement

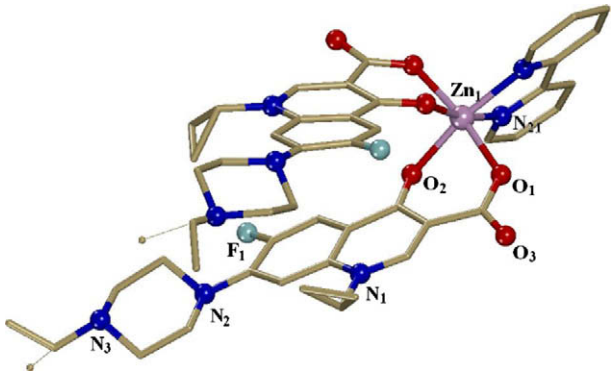

Figure 3. A drawing of the molecular structure of **3** with only the heteroatoms labeling.

similar with that observed in a similar zinc complex, [Zn(erx)$_2$(py)$_2$], reported earlier.[17]

2.3. DNA binding study by UV spectroscopy

The study of the interaction of quinolones and their complexes with DNA is of great importance since their activity as antibacterial drugs is focused on the inhibition of DNA replication[29] by targeting essential type II bacterial topoisomerases such as DNA gyrase and topoisomerase IV.[16] DNA can provide three distinctive binding sites for quinolone metal complexes (groove binding, electrostatic binding to phosphate group and intercalation).[30–32]

The changes observed in the UV spectra upon titration may give evidence of the existing interaction mode, since a hypochromism due to $\pi\rightarrow\pi^*$ stacking interactions may appear in the case of the intercalative binding mode,[33] while red-shift (bathochromism) may be observed when the DNA duplex is stabilized.[34]

The UV spectra have been recorded for a constant CT DNA concentration in different [compound]/[DNA] mixing ratios (r). UV spectra of CT DNA in the presence of a complex derived for diverse r values are shown representatively for **2** in Figure 4. The intensity at λ_{max} = 258 nm remains almost stable and is accompanied by a red-shift of the λ_{max} up to 266 nm for all complexes, indicating that their interaction with CT DNA results in the direct formation of a new complex with double-helical CT DNA. The observed red-shift is an evidence of the stabilization of the CT DNA duplex.[33] The interaction of Herx with CT DNA studied has exhibited a red-shift the band λ_{max} = 258 nm up to 267 nm.[17]

In Figure 5, the changes occurred in the spectrum of a 10^{-5} M solution of **1**–**3** upon addition of CT DNA in diverse r values can be observed. In the UV region, the intense absorption bands observed in the spectra of Herx and the complexes are attributed to the intra-ligand $\pi\rightarrow\pi^*$ transition of the coordinated groups of enrofloxacinato ligands.[17,18] Any interaction between each complex and CT DNA could perturb the intra-ligand centred spectral transitions.[20,35,36]

In the UV spectrum of **1**, the band centered at 326 nm exhibits a hyperchromism (Fig. 5A) accompanied with a blue-shift of 2 nm (up to 324 nm). The observed hyperchromic effect suggests binding to CT DNA attributed either to external contact (electrostatic or groove binding) or to the fact that **1** could uncoil the helix structure of DNA resulting in a destabilization of the DNA duplex.[37]

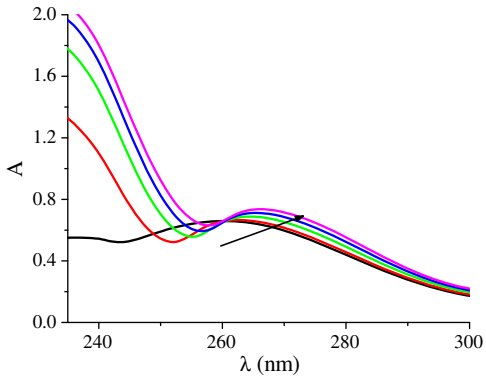

Figure 4. UV spectra of CT DNA in buffer solution (150 mM NaCl and 15 mM trisodium citrate at pH 7.0) in the absence or presence of [Zn(erx)$_2$(phen)]·4MeOH, **2**·4MeOH. The arrows show the changes upon increasing amounts of complex.

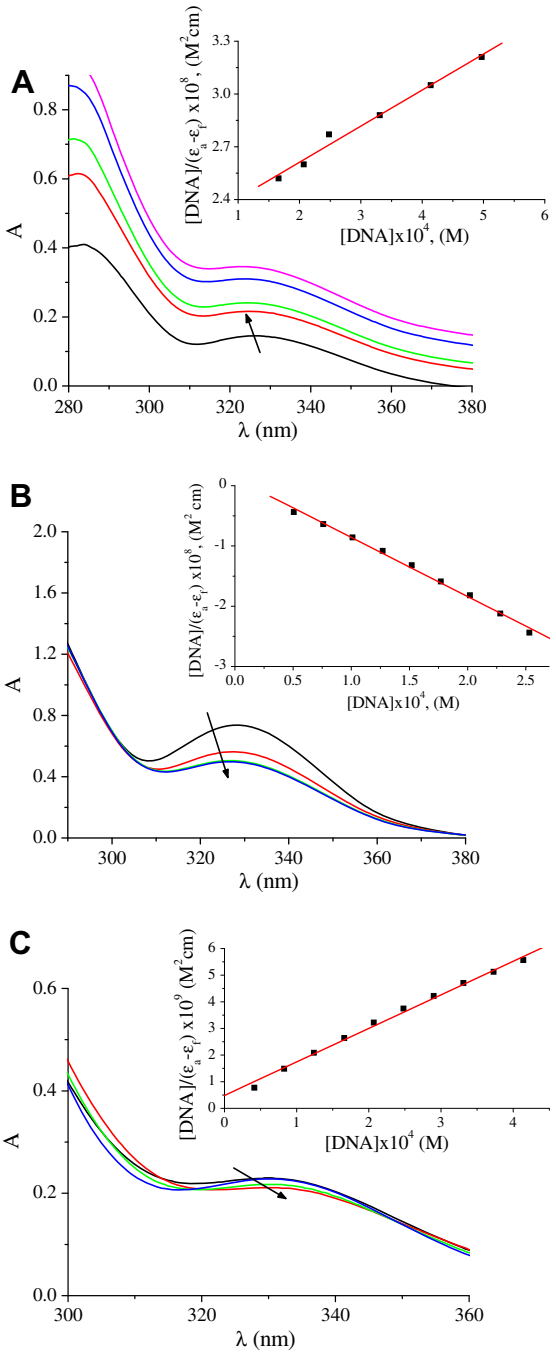

Figure 5. UV spectra of (A) [Zn(erx)$_2$(H$_2$O)$_2$] **1**, (B) [Zn(erx)$_2$(phen)]·4MeOH, **2**·4MeOH and (C) [Zn(erx)$_2$(bipy)] **3**, in dmso ([Complex] = 10 μM) solution in the presence of CT DNA at increasing amounts. The arrows show the changes upon increasing amounts of CT DNA. Inset: plot of $\frac{[DNA]}{(\varepsilon_A-\varepsilon_f)}$ versus [DNA].

In the UV spectrum of **2**, the band centered at 328 nm exhibits a significant hypochromism of 30% (Fig. 5B) suggesting tight binding to CT DNA, maybe by intercalation. A distinct isosbestic point at ~300 nm appears upon addition of CT DNA.

For complex **3**, the band centered at 328 nm exhibits a less pronounced hypochromism of ~10% upon addition of CT DNA accompanied with a red-shift of 4 nm up 332 nm (Fig. 5C) indicative of DNA-stabilization and tight binding possibly by intercalation.

The results derived from the UV titration experiments suggest that all complexes can bind tightly to CT DNA. The possibility of intercalation for **2** and **3** cannot be ruled out and, especially for **2,** is enhanced due to the co-existence in the molecule of the intercalating agent phenanthroline.[20]

The intrinsic binding constant K_b can be obtained by monitoring the changes in the absorbance at the corresponding λ_{max} with increasing concentrations of CT DNA and is given by the ratio of slope to the y intercept in plots $\frac{[DNA]}{(\varepsilon_a-\varepsilon_f)}$ versus [DNA] (insets in Fig. 4), according to the following equation:[33]

$$\frac{[DNA]}{(\varepsilon_a-\varepsilon_f)}=\frac{[DNA]}{(\varepsilon_b-\varepsilon_f)}+\frac{1}{K_b(\varepsilon_b-\varepsilon_f)} \quad (3)$$

where [DNA] is the concentration of DNA in base pairs, $\varepsilon_a = A_{obsd}/[complex]$, ε_f = the extinction coefficient for the free complex and ε_b = the extinction coefficient for the complex in the fully bound form, respectively. The calculated K_b values for Herx and complexes are cited in Table 2. The K_b values suggest a relatively moderate binding of Herx and **1–3** to CT DNA. The K_b value obtained for **2** ($=8.03(\pm0.06)\times10^4\ M^{-1}$) is much higher than the other compounds. This can be attributed to the co-existence of a phenanthroline ligand, which is capable to intercalate to the DNA bases. The K_b values for Herx, **1** and **3** are of lower magnitude than that of the typical indicator of intercalation EB, while the K_b of **2** is relatively close to the EB binding affinity for CT DNA, ($K_b = 1.23(\pm0.07)\times10^5\ M^{-1}$), suggesting that electrostatic and/or intercalative interaction may affect EB displacement from the EB–DNA complex.[38]

2.4. Competitive studies with ethidium bromide

The ability of the compounds to displace EB (=3,8-diamino-5-ethyl-6-phenyl-phenanthridinium bromide) from its EB–DNA complex can be examined through a competitive EB binding study with fluorescence experiments.[20] EB is a phenanthridine fluorescence dye and is a typical indicator of intercalation, forming soluble complexes with nucleic acids and emitting intense fluorescence in the presence of CT DNA due to the intercalation of the planar phenanthridinium ring between adjacent base pairs on the double helix.[39] The changes observed in the spectra of EB on its binding to CT DNA are often used for the interaction study between DNA and other compounds, such as metal complexes.[40]

Herx and complexes **1–3** show no fluorescence at room temperature in solution or in the presence of CT DNA, and their binding to DNA cannot be directly predicted through the emission spectra and competitive EB binding studies are performed in order to further investigate the binding of each compound with DNA. EB does not show any appreciable emission in buffer solution due to fluorescence quenching of the free EB by the solvent molecules.[41] Upon addition of Herx or complexes **1–3** to a solution containing EB, neither quenching of free EB fluorescence has been observed nor new peaks in the spectra appear. EB fluorescence intensity is highly enhanced upon addition of CT DNA, due to its strong intercalation between the adjacent DNA base pairs.[41] Addition of a second molecule, which can bind to DNA more strongly than EB results in a decrease the DNA-induced EB emission due to the replacement of EB, and/or electron transfer.[42]

The emission spectra of EB bound to CT DNA in the absence and presence of each compound have been recorded for [EB] = 2×10^{-5} M, [DNA] = 2.5×10^{-5} M for increasing amounts of each compound. The addition of Herx and complexes **1–3** results in a decrease of the intensity of the emission band at 592 nm of the DNA–EB system upon addition of each compound at diverse *r* values (Fig. 6A) (up to 64% of the initial EB–DNA fluorescence intensity for Herx, 56% for **1,** 40% for **2** and 35% for **3**) indicating the competition of the compounds with EB in binding to DNA. The observed quenching of DNA–EB fluorescence especially for complexes **2** and **3** suggests that they displace EB from the DNA–EB complex and they can interact with CT DNA probably by the intercalative mode.[35,43–45]According to linear Stern–Volmer equation:[20,46]

$$\frac{Io}{I}=1+K_{SV}[Q] \quad (4)$$

where Io and *I* are the emission intensities in the absence and the presence of the quencher, respectively, [Q] is the concentration of the quencher (Herx or complexes **1–3**) and K_{SV} is the Stern–Volmer constant which can be obtained by the slope of the diagram $\frac{Io}{I}$ vs [Q] (Fig. 6B) and is often used to evaluate the quenching efficiency for

Table 2
The DNA binding constants (K_b) and the Stern–Volmer constants (K_{SV}) of Herx and complexes **1–3**

Compound	K_b (M^{-1})	K_{SV} (M^{-1})
Herx[17]	$1.69(\pm0.04)\times10^3$	$1.91(\pm0.07)\times10^5$
$[Zn(erx)_2(H_2O)_2]$, **1**	$9.32(\pm0.32)\times10^2$	$2.33(\pm0.09)\times10^5$
$[Zn(erx)_2(phen)]\cdot4MeOH$, **2**·4MeOH	$8.03(\pm0.06)\times10^4$	$4.31(\pm0.20)\times10^5$
$[Zn(erx)_2(bipy)]$, **3**	$2.61(\pm0.20)\times10^4$	$5.88(\pm0.19)\times10^5$

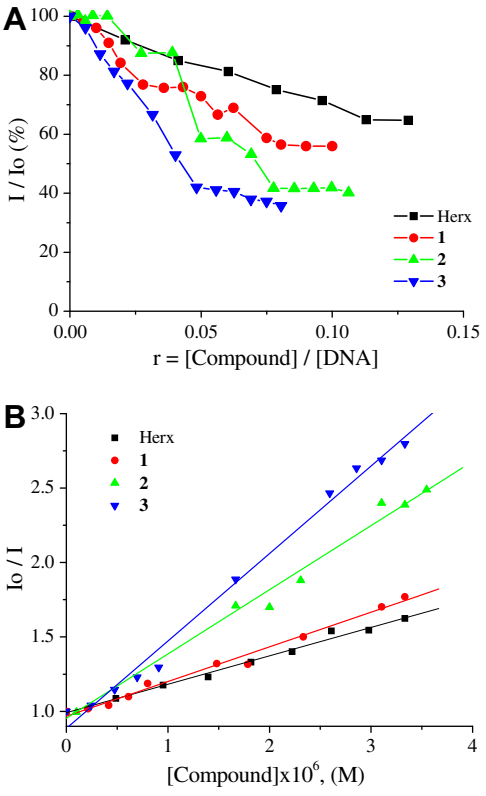

Figure 6. (A) Plot of % EB relative fluorescence intensity at λ_{em} = 592 nm (%) versus *r* (*r* = [compound]/[DNA]) for Herx and complexes **1–3** in buffer solution (150 mM NaCl and 15 mM trisodium citrate at pH 7.0). (B) Stern–Volmer plot for Herx and complexes **1–3** in buffer solution (150 mM NaCl and 15 mM trisodium citrate at pH 7.0).

each compound. The Stern–Volmer plot illustrates that the quenching of EB bound to DNA by Herx or complex **1**–**3** is in good agreement ($R = 0.99$) with (Eq. 4), which proves that the partial replacement of EB bound to DNA results in a decrease in the fluorescence intensity.[44,45] The relatively high K_{SV} values (Table 2) of the complexes show that they can displace EB and bind to the DNA.[17,20,35,36,44]

2.5. Binding of serum albumins

Serum albumins are proteins involved in the transport of metal ions and metal complexes with drugs through the blood stream. The interaction of Herx and complexes **1**–**3** with HSA and BSA has been studied from tryptophan emission-quenching experiments.

HSA contains 585 amino acid residues with only one tryptophan located at position 214 along the chain, in subdomain IIA.[47] HSA binds reversibly to a large number of endogenous and exogenous compounds. HSA solutions when excited at 295 nm show a strong fluorescence emission with a peak at 351 nm due to the single tryptophan residue.[48] Herx and complexes **1**–**3** in buffer solutions exhibit a maximum emission at 410 nm under the same experimental conditions and the SA fluorescence spectra have been corrected before the experimental data processing. The changes in the emission spectra of tryptophan in HSA are primarily due to changes in protein conformation, subunit association, substrate binding or denaturation.[49] Addition of Herx or complexes **1**–**3** to HSA leads to a decrease of the fluorescence signal at 351 nm with the simultaneous appearance of an isoemissive point at 379 nm (Fig. 7A). The quenching provoked by Herx and the complexes (Fig. 7B) is significant (up to 54% of the initial fluorescence intensity for Herx, 62% for **1**, 45% for **2** and 39% for **3**) because of possible changes in protein secondary structure leading to changes in tryptophan environment of HSA.[50] These results clearly indicate the binding of Herx or each complex to HSA, which quenches the intrinsic fluorescence of the single tryptophan in HSA. The Stern–Volmer and Scatchard graphs may be used in order to study the interaction of a quencher in presence of serum albumins. According to Stern–Volmer quenching equation:[47]

$$\frac{Io}{I} = 1 + k_q t_0[Q] = 1 + K_{SV}[Q] \quad (5)$$

where Io = the initial tryptophan fluorescence intensity of SA, I = the tryptophan fluorescence intensity of SA after the addition of the quencher, k_q = the quenching rate constants SA, K_{SV} = the dynamic quenching constant, τ_o = the average lifetime of SA without the quencher, [Q] = the concentration of the quencher and $K_{SV} = k_q\tau_o$. Taking as fluorescence lifetime (τ_o) of tryptophan in SA at around 10^{-8} s,[51] the dynamic quenching constant (K_{SV}, M^{-1}) can be obtained by the slope of the diagram $\frac{Io}{I}$ versus [Q] (Fig. S1)), and subsequently the approximate quenching constant (k_q, $M^{-1}\,s^{-1}$) may be calculated. The calculated values for the interaction of Herx and complexes **1**–**3** with HSA are given in Table 3 and indicate good HSA binding propensity of the complexes. The k_q values increase in the order **1** < Herx < **2** < **3** with complex **3** exhibiting the strongest protein-binding ability. The k_q values ($>10^{12}\,M^{-1}\,s^{-1}$) are higher than diverse kinds of quenchers for biopolymers fluorescence ($2.0 \times 10^{10}\,M^{-1}\,s^{-1}$) indicating that a static quenching mechanism may be operative.[52] Using the Scatchard equation:

$$\frac{\frac{\Delta I}{Io}}{[Q]} = nK - K\frac{\Delta I}{Io} \quad (6)$$

where n is the number of binding sites per albumin and K is the association binding constant, K (M^{-1}) may be calculated from the slope in plots $\frac{\frac{\Delta I}{Io}}{[Q]}$ versus $\frac{\Delta I}{Io}$ (Fig. S2) and n is given by the ratio of y intercept to the slope.[52] It is obvious that Herx (Table 4) exhibits the highest K value, suggesting that the coordination of Herx to Zn(II) results in a decreased affinity for HSA. On the other hand, the n value of Herx increases when it is coordinated to Zn(II) in complexes **1**–**3**.

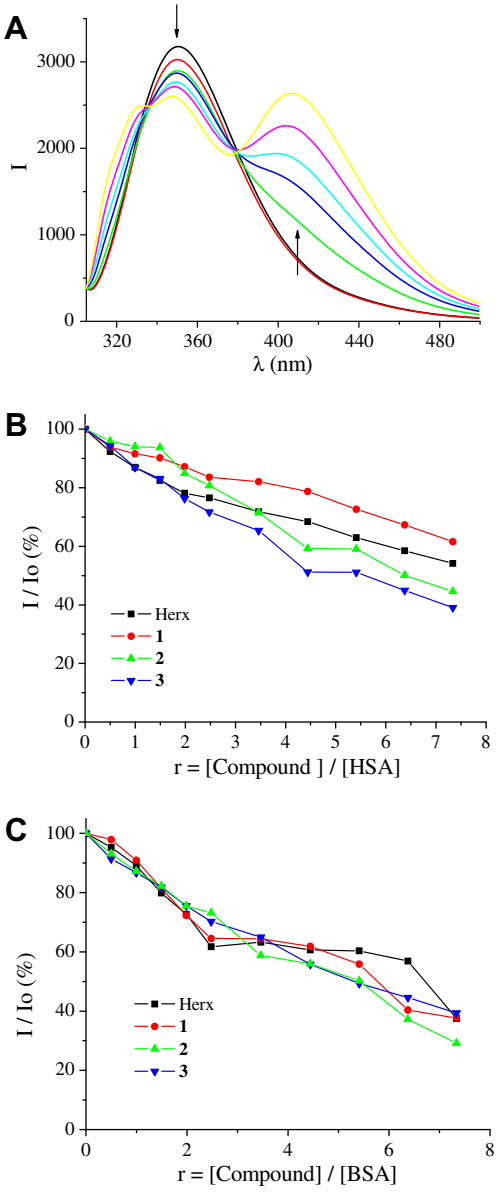

Figure 7. (A) Emission spectra ($\lambda_{exit} = 295$ nm) for HSA ([HSA] = 3 μM) in buffer solution in the absence and presence of increasing amounts of complex **2** (r = [**2**]/[HSA] = 0–8). The arrow shows the changes of intensity upon increasing amounts of **2**. (B) Plot of % relative fluorescence intensity at $\lambda_{em} = 351$ nm (%) versus r (r = [compound]/[HSA]) for Herx and complexes **1**–**3** in buffer solution (150 mM NaCl and 15 mM trisodium citrate at pH 7.0). (C) Plot of % relative fluorescence intensity at $\lambda_{em} = 343$ nm (%) versus r (r = [compound]/[BSA]) for Herx and complexes **1**–**3** in buffer solution (150 mM NaCl and 15 mM trisodium citrate at pH 7.0).

BSA is the most extensively studied serum albumin, due to its structural homology with HSA.[47] BSA has two tryptophans, Trp-134 and Trp-212, embedded in the first subdomain IB and subdomain IIA, respectively. BSA solutions exhibit a strong fluorescence emission with a peak at 343 nm due to the tryptophan residues, when excited at 295 nm.[48] Addition of Herx or complexes **1**–**3** to BSA (Fig. 7C) results in a fluorescence quenching (up to 37% of the initial fluorescence intensity of BSA for Herx, 38% for **1**, 29% for **2** and 39% for **3**) due to possible changes in protein secondary

Table 3
The HSA binding constants and parameters derived for Herx and complexes **1**–**3**

Compound	K_{SV} (M^{-1})	k_q (M^{-1} s^{-1})	K (M^{-1})	n
Herx	$3.56(\pm0.11)\times10^4$	$3.56(\pm0.11)\times10^{12}$	$7.63(\pm0.23)\times10^4$	0.71
$[Zn(erx)_2(H_2O)_2]$, **1**	$2.27(\pm0.13)\times10^4$	$2.27(\pm0.13)\times10^{12}$	$3.73(\pm0.18)\times10^4$	0.82
$[Zn(erx)_2(phen)]\cdot4MeOH$, **2**·4MeOH	$5.66(\pm0.40)\times10^4$	$5.66(\pm0.40)\times10^{12}$	$3.38(\pm0.11)\times10^4$	1.29
$[Zn(erx)_2(bipy)]$, **3**	$6.94(\pm0.33)\times10^4$	$6.94(\pm0.33)\times10^{12}$	$3.39(\pm0.20)\times10^4$	1.39

Table 4
The BSA binding constants and parameters derived for Herx and complexes **1**–**3**

Compound	K_{SV} (M^{-1})	k_q (M^{-1} s^{-1})	K (M^{-1})	n
Herx	$4.48(\pm0.40)\times10^4$	$4.48(\pm0.40)\times10^{12}$	$1.82(\pm0.15)\times10^4$	1.14
$[Zn(erx)_2(H_2O)_2]$, **1**	$6.98(\pm0.23)\times10^4$	$6.98(\pm0.23)\times10^{12}$	$2.78(\pm0.18)\times10^4$	1.63
$[Zn(erx)_2(phen)]\cdot4MeOH$, **2**·4MeOH	$6.29(\pm0.29)\times10^4$	$6.29(\pm0.29)\times10^{12}$	$2.09(\pm0.11)\times10^4$	2.20
$[Zn(erx)_2(bipy)]$, **3**	$6.82(\pm0.26)\times10^4$	$6.82(\pm0.26)\times10^{12}$	$3.89(\pm0.22)\times10^4$	1.32

structure of BSA indicating the binding of Herx or each complex to BSA.[51] An isoemissive point appears at 380 nm (Fig. S3).

The Stern–Volmer equation applied for the interaction with BSA (Fig. S4) shows that the curves have fine linear relationships ($r = 0.99$) according to Eq. 5. The calculated values of K_{sv} and k_q for the interaction of Herx and complexes **1**–**3** with BSA as given in Table 4 indicate good BSA binding propensity of the complexes. The k_q value of Herx increases upon coordination to Zn(II) with **1** exhibiting the strongest protein-binding ability.

From the Scatchard graph (Fig. S5) and Eq. 6, the association binding constant of each compound has been calculated (Table 4). The K value of Herx is relatively high and increases slightly when it is bound to Zn(II) as found for complexes **1**–**3** with complex **3** exhibiting the highest K value. The n value of Herx increases when it is coordinated to Zn(II) either in the absence or in the presence of the N-donor ligands (Table 4) with **2** exhibiting the highest value.

Comparing the affinity of the compounds for HSA and BSA, it is evident that Herx, **1** and **2** show higher affinity for HSA than BSA, while **3** exhibits similar binding constant for BSA and HSA.

3. Conclusions

The synthesis and characterization of the neutral mononuclear zinc complexes with the second-generation quinolone antibacterial drug enrofloxacin in the absence or presence of the N,N′-donor heterocyclic ligands 1,10-phenanthroline or 2,2′-bipyridine has been realized. In these complexes, the enrofloxacinato ligands are bound to zinc(II) via the ketone oxygen and a carboxylato oxygen. The crystal structure of the complex $Zn(erx)_2(phen)$ has been determined by X-ray crystallography revealing a distorted octahedral geometry for Zn(II).

The interaction of these complexes with CT DNA has been studied with UV spectroscopy revealing their ability to bind to DNA. UV spectroscopic titrations have been used in order to calculate the binding constant K_b of the complexes with CT DNA. $[Zn(erx)_2(phen)]$ exhibits the highest K_b value among all the compounds examined, which is comparable to the K_b value of EB.

Competitive binding studies with EB have been performed with fluorescence spectroscopy, showing that the interaction between DNA–EB complex and the complexes releases EB from its DNA complex, indicating that the complexes can bind to DNA probably via the intercalative mode.

Enrofloxacin and its Zn(II) complexes show good binding affinity to BSA and HSA proteins giving relatively high binding constants. Especially, Herx and complexes **1**–**2** exhibit higher affinity for HSA than BSA.

4. Experimental

4.1. Materials—instrumentation—physical measurements

Enrofloxacin, CT DNA, BSA, HSA and EB were purchased from Sigma, NaCl and all solvents were purchased from Merck, trisodium citrate was purchased from Riedel-de Haen and $ZnCl_2$, bipy, phen and KOH were purchased from Aldrich Co. All the chemicals and solvents were reagent grade and were used as purchased.

DNA stock solution was prepared by dilution of CT DNA to buffer (containing 150 mM NaCl and 15 mM trisodium citrate at pH 7.0) followed by exhaustive stirring at 4 °C for three days, and kept at 4 °C for no longer than a week. The stock solution of CT DNA gave a ratio of UV absorbance at 260 and 280 nm (A_{260}/A_{280}) of 1.89, indicating that the DNA was sufficiently free of protein contamination.[53] The DNA concentration was determined by the UV absorbance at 260 nm after 1:20 dilution using $\varepsilon = 6600\ M^{-1}\ cm^{-1}$.[54]

Infrared (IR) spectra (400–4000 cm^{-1}) were recorded on a Nicolet FT-IR 6700 spectrometer with samples prepared as KBr pellets. UV–vis (UV–vis) spectra were recorded as nujol mulls and in solution at concentrations in the range 10^{-5}–10^{-3} M on a Hitachi U-2001 dual beam spectrophotometer. C, H and N elemental analysis were performed on a Perkin–Elmer 240B elemental analyzer. Molecular conductivity measurements were carried out with a Crison Basic 30 conductometer. Fluorescence spectra were recorded in solution on a Hitachi F-7000 fluorescence spectrophotometer.

4.2. Synthesis of the complexes

4.2.1. $[Zn(erx)_2(H_2O)_2]$, 1

Complex **1** was prepared by the addition of a methanolic solution (15 mL) of enrofloxacin (0.4 mmol, 144 mg), deprotonated with KOH (0.4 mmol, 22 mg), to a methanolic solution (10 mL) of $ZnCl_2$ (0.2 mmol, 28 mg). The reaction mixture was refluxed for 1 h. The solution was filtered and left for slow evaporation. After a few days a pale yellow microcrystalline solid was deposited and collected with filtration. Yield: 115 mg, 65%. Anal. Calcd for $[Zn(erx)_2(H_2O)_2]$ ($C_{38}H_{46}F_2N_6O_8Zn$) (MW = 818.20): C, 55.78; H, 5.67; N, 10.27. Found: C, 55.41; H, 5.83; N, 10.13. IR: ν_{max}/cm^{-1} $\nu(C{=}O)_{ket}$ 1629(vs); $\nu_{asym}(CO_2)$: 1581(vs); $\nu_{sym}(CO_2)$: 1380(vs); $\Delta = \nu_{asym}(CO_2) - \nu_{sym}(CO_2)$: 201 cm^{-1} (KBr pellet); The complex is soluble in DMSO and DMF and is non-electrolyte.

4.2.2. $[Zn(erx)_2(phen)]\cdot4MeOH$, 2·4MeOH

A methanolic solution (15 mL) of enrofloxacin (0.4 mmol, 144 mg), deprotonated with KOH (0.4 mmol, 22 mg), and a metha-

nolic solution of phen (0.2 mmol, 36 mg) were added simultaneously and slowly to a methanolic solution (10 mL) of $ZnCl_2$ (0.2 mmol, 28 mg). The resulting reaction mixture was stirred for 2 h, reduced in volume and left for slow evaporation. Pale yellow crystals of [Zn(erx)$_2$(phen)]·4MeOH, **2**·4MeOH, suitable for X-ray structure determination were deposited over two days. Yield: 135 mg, 65%. Anal. Calcd for [Zn(erx)$_2$(phen)]·4MeOH ($C_{54}H_{66}F_2N_8O_{10}Zn$) (MW = 1090.54): C, 59.47; H, 6.10; N, 10.27. Found: C, 59.75; H, 5.95; N, 10.22. IR: ν_{max}/cm^{-1} $\nu(C{=}O)_{ket}$ 1637(vs); $\nu_{asym}(CO_2)$: 1616(vs); $\nu_{sym}(CO_2)$: 1376(vs); $\Delta = \nu_{asym}(CO_2) - \nu_{sym}(CO_2)$: 240 cm^{-1} (KBr pellet); The complex is soluble in dmso and dmf, partially in H_2O and ethanol and is non-electrolyte.

4.2.3. [Zn(erx)$_2$(bipy)], 3

Complex **3** was prepared in a similar way. Bipy (0.2 mmol, 31 mg) was used instead. Pale yellow crystalline product of [Zn(erx)$_2$(bipy)], **3**, was deposited over eight days. Yield: 130 mg, 70%. Anal. Calcd for [Zn(erx)$_2$(bipy)] ($C_{48}H_{50}F_2N_8O_6Zn$) (MW = 938.35): C, 61.44; H, 5.37; N, 11.94. Found: C, 61.30; H, 5.29; N, 11.59. IR: ν_{max}/cm^{-1} $\nu(C{=}O)_{ket}$ 1636(vs); $\nu_{asym}(CO_2)$: 1612(vs); $\nu_{sym}(CO_2)$: 1375(vs); $\Delta = \nu_{asym}(CO_2) - \nu_{sym}(CO_2)$: 237 cm^{-1} (KBr pellet); The complex is soluble in dmf and dmso, partially in H_2O and ethanol and is non-electrolyte.

4.3. DNA binding studies

The interaction of complexes **1**–**3** with CT DNA has been studied with UV spectroscopy in order to investigate the possible binding modes to CT DNA and to calculate the binding constants to CT DNA (K_b). In UV titration experiments, the spectra of CT DNA in the presence of each complex have been recorded for a constant CT DNA concentration in diverse [complex]/[CT DNA] mixing ratios (r).

The competitive studies of each compound with EB have been investigated with fluorescence spectroscopy in order to examine whether the compound is able to displace EB from its CT DNA–EB complex. The CT DNA–EB complex was prepared by adding 20 μM EB and 26 μM CT DNA in buffer (150 mM NaCl and 15 mM trisodium citrate at pH 7.0). The intercalating effect of complexes **1**–**3** with the DNA–EB complex was studied by adding a certain amount of a solution of the compound step by step into the solution of the DNA–EB complex. The influence of the addition of each compound to the DNA–EB complex solution has been obtained by recording the variation of fluorescence emission spectra. The influence of the addition of each compound to the DNA–EB complex solution has been obtained by recording the variation of fluorescence emission spectra.

4.4. Serum albumin (SA) binding studies

The protein binding study was performed by tryptophan fluorescence quenching experiments using human (HSA, 3 μM) or bovine (BSA, 3 μM) serum albumin in buffer (containing 15 mM trisodium citrate and 150 mM NaCl at pH 7.0). The quenching of the emission intensity of tryptophan residues of HSA at 351 nm or BSA at 343 nm was monitored using Herx or complexes **1**–**3** as quenchers with increasing concentration.[47,48] Fluorescence spectra were recorded from 300 to 500 nm at an excitation wavelength of 296 nm. The fluorescence spectra of Herx and complexes **1**–**3** in buffer solutions were recorded under the same experimental conditions and exhibited a maximum emission at 410 nm. Therefore, the quantitative studies of the serum albumin fluorescence spectra were performed after their correction by subtracting the spectra of the compounds.

Table 5
Crystallographic data for complex **2**·4**MeOH**

	2·4MeOH
Formula	$C_{54}H_{66}F_2N_8O_{10}Zn$
Fw	1090.52
T (K)	298
Crystal system	Monoclinic
Space group	$C2c$
a	15.714(9)
b	33.227(9)
c	10.608(2)
α	90.00
β	99.853(9)
γ	90.00
Volume	5457(4)
Z	4
D(calc) (Mg/m^3)	1.327
Abs. coef., μ (mm^{-1})	0.521
F(0 0 0)	2296
θ range	2.24–25.00
GOF on F^2	1.040
R_1	0.0626[a]
wR_2	0.1653[a]

[a] 3118 Reflections with $I > 2\sigma(I)$.

4.5. X-ray crystal structure determination

Slow crystallization from methanol yielded colorless prismatic crystals of **2**·4**MeOH**. A crystal with approximate dimensions 0.15 × 0.15 × 0.75 mm was mounted in capillary. Diffraction measurements were made on a Crystal Logic Dual Goniometer diffractometer using graphite monochromated Mo radiation. Unit cell dimensions were determined and refined by using the angular settings of 25 automatically centered reflections in the range $11 < 2\theta < 23°$ and they appear in Table 5. Intensity data were recorded using a $\theta - 2\theta$ scan. Three standard reflections monitored every 97 reflections showed less than 3% variation and no decay. Lorentz, polarization corrections were applied using Crystal Logic software. The crystals of **3** were very small in size, showed poor diffraction ability and very weak intensities only at lower theta values. Repeating efforts to improve the quality and size of the crystals proved unsuccessful, thus only the gross structure was established. A colorless crystal of **3** (0.07 × 0.09 × 0.26 mm) was taken directly from the mother liquor and immediately cooled to −93 °C. Diffraction measurements were made on a Rigaku R-AXIS SPIDER Image Plate diffractometer using graphite monochromated Cu Kα (Mo Kα) radiation. Data collection (ω-scans) and processing (cell refinement, data reduction and Empirical absorption correction) were performed using the CRYSTALCLEAR program package.[55] The structures were solved by direct methods using[56] SHELXS-97 and refined by full-matrix least-squares techniques on F^2 with SHELXL-97.[57] Further experimental crystallographic details for **2**·4**MeOH**: $2\theta_{max} = 50°$; reflections collected/unique/used, 5093/4817 [R_{int} = 0.0161]/4817; 442 parameters refined; $(\Delta/\sigma)_{max} = 0.000$; $(\Delta\rho)_{max}/(\Delta\rho)_{min} = 0.468/-0.239$ e/Å^3; R_1/wR_2 (for all data), 0.1077/0.1946. All hydrogen atoms were located by difference maps and were refined isotropically, except those on C18 which were introduced at calculated positions as riding on bonded atoms. All non-hydrogen atoms were refined anisotropically. Further experimental crystallographic details for **3**·0.5MeOH·3H$_2$O: $C_{48.5}H_{58}F_2N_8O_{9.5}Zn$, fw = 1008.40, a = 15.3734(9), b = 32.736(2), c = 10.5630(6) Å, β = 99.507(1)°, V = 5243.0(5) Å^3, Z = 4, space group $C2/c$, $2\theta max = 48°$; reflections collected/unique/used, 17542/4069 [R_{int} = 0.0709]/4069; 325 parameters refined; $(\Delta\sigma)_{max} = 0.003$; $(\Delta\rho)_{max}/(\Delta\rho)_{min} = 1.092/-0.562$ e/Å^3; R/R_w (3234 reflections with $I > 2\sigma(I)$), 0.0948/0.2678; R/R_w (for all data), 0.1096/0.2813. All hydrogen atoms were introduced at calculated

positions as riding on bonded atoms; all non-H atoms were refined anisotropically.

Supplementary data

Supplementary data associated with this article can be found, in the online version, at doi:10.1016/j.bmc.2010.02.021.

References and notes

1. Farrell, N. *Coord. Chem. Rev.* **2002**, *232*, 1.
2. Walkup, G. K.; Burdette, S. C.; Lippard, S. J.; Tsien, R. Y. *J. Am. Chem. Soc.* **2000**, *122*, 5644.
3. Di Vaira, M.; Bazzicalupi, C.; Orioli, P.; Messori, L.; Bruni, B.; Zatta, P. *Inorg. Chem.* **2004**, *43*, 3795.
4. d'Angelo, J.; Morgant, G.; Ghermani, N. E.; Desmaele, D.; Fraisse, B.; Bonhomme, F.; Dichi, E.; Sghaier, M.; Li, Y.; Journaux, Y.; Sorenson, J. R. J. *Polyhedron* **2008**, *27*, 537.
5. Sakurai, H.; Kojima, Y.; Yoshikawa, Y.; Kawabe, K.; Yasui, H. *Coord. Chem. Rev.* **2002**, *226*, 187.
6. Zhou, Q.; Hambley, T. W.; Kennedy, B. J.; Lay, P. A.; Turner, P.; Warwick, B.; Biffin, J. R.; Regtop, H. L. *Inorg. Chem.* **2000**, *39*, 3742.
7. Kasuga, N. C.; Sekino, K.; Ishikawa, M.; Honda, A.; Yokoyama, M.; Nakano, S.; Shimada, N.; Koumo, C.; Nomiya, K. *J. Inorg. Biochem.* **2003**, *96*, 298.
8. Belicchi Ferrari, M.; Bisceglie, F.; Pelosi, G.; Tarasconi, P.; Albertini, R.; Pinelli, S. *J. Inorg. Biochem.* **2001**, *87*, 137.
9. Travnicek, Z.; Krystof, V.; Sipl, M. *J. Inorg. Biochem.* **2006**, *100*, 214.
10. Casas, J. S.; Castellano, E. E.; Couce, M. D.; Ellena, J.; Sanchez, A.; Sordo, J.; Taboada, C. *J. Inorg. Biochem.* **2006**, *100*, 124.
11. Li, Z.; Wu, F.; Gong, Y.; Hu, C.; Zhang, Y.; Gan, M. *Chin. J. Chem.* **2007**, *25*, 1809.
12. Turel, I. *Coord. Chem. Rev.* **2002**, *232*, 27.
13. Souza, M. J.; Bittencourt, C. F.; Morsch, L. M. *J. Pharm. Biomed. Anal.* **2002**, *28*, 1197.
14. Boothe, D. M. *Vet. Med.* **1994**, *89*, 744.
15. Ameyama, S.; Shinmura, Y.; Takahata, M. *Antimicrob. Agents Chemother.* **2003**, *47*, 2327.
16. King, D. E.; Malone, R.; Lilley, S. H. *Am. Fam. Physician* **2000**, *61*, 2741.
17. Tarushi, A.; Psomas, G.; Raptopoulou, C. P.; Psycharis, V.; Kessissoglou, D. P. *Polyhedron* **2009**, *28*, 3272.
18. Efthimiadou, E. K.; Katsarou, M.; Sanakis, Y.; Raptopoulou, C. P.; Karaliota, A.; Katsaros, N.; Psomas, G. *J. Inorg. Biochem.* **2006**, *100*, 1378.
19. Recillas-Mota, J.; Flores-Alamo, M.; Moreno-Esparza, R.; Gracia-Mora, J. *Acta Crystallogr., Sect. E* **2007**, *63*, m3030.
20. Tarushi, A.; Psomas, G.; Raptopoulou, C. P.; Kessissoglou, D. P. *J. Inorg. Biochem.* **2009**, *103*, 898.
21. Nakamoto, K. *Infrared and Raman Spectra of Inorganic and Coordination Compounds*, 4th ed.; Wiley: New York, 1986.
22. Chen, Z.; Xiong, R.; Zhang, J.; Chen, X.; Xue, Z.; You, X. *Inorg. Chem.* **2001**, *40*, 4075.
23. Xiao, D.; Wang, E.; An, H.; Su, Z.; Li, Y.; Gao, L.; Sun, C.; Xu, L. *Chem. Eur. J.* **2005**, *11*, 6673.
24. Ruiz, M.; Ortiz, R.; Perello, L.; Castineiras, A.; Quiros, M. *Inorg. Chim. Acta* **1993**, *211*, 133.
25. Lopez-Gresa, M. P.; Ortiz, R.; Perello, L.; Latorre, J.; Liu-Gonzalez, M.; Garcia-Granda, S.; Perez-Priede, M.; Canton, E. *J. Inorg. Biochem.* **2002**, *92*, 65.
26. Turel, I.; Gruber, K.; Leban, I.; Bukovec, N. *J. Inorg. Biochem.* **1996**, *61*, 197.
27. Frenz, B. A.; Ibers, J. A. *Inorg. Chem.* **1972**, *11*, 1109.
28. Grirrane, A.; Pastor, A.; Ienco, A.; Mealli, C.; Galindo, A. *J. Chem. Soc., Dalton Trans.* **2002**, 3771.
29. Son, G.; Yeo, J.; Kim, M.; Kim, S.; Holmen, A.; Akerman, B.; Norden, B. *J. Am. Chem. Soc.* **1998**, *120*, 6451–6457.
30. Drevensek, P.; Poklar Ulrih, N.; Majerle, A.; Turel, I. *J. Inorg. Biochem.* **2006**, *100*, 1705.
31. Vilfan, I. D.; Drevensek, P.; Turel, I.; Poklar Ulrih, N. *Biochim. Biophys. Acta, Gene Struct. Expr.* **2003**, *1628*, 111.
32. Song, Y.; Wu, Q.; Yang, P.; Luan, N.; Wang, L.; Liu, Y. *J. Inorg. Biochem.* **2006**, *100*, 1685.
33. Pyle, A. M.; Rehmann, J. P.; Meshoyrer, R.; Kumar, C. V.; Turro, N. J.; Barton, J. K. *J. Am. Chem. Soc.* **1989**, *111*, 3053.
34. Long, E. C.; Barton, J. K. *Acc. Chem. Res.* **1990**, *23*, 271.
35. Skyrianou, K. C.; Efthimiadou, E. K.; Psycharis, V.; Terzis, A.; Kessissoglou, D. P.; Psomas, G. *J. Inorg. Biochem.* **2009**, *103*, 1617.
36. Skyrianou, K. C.; Perdih, F.; Turel, I.; Kessissoglou, D. P.; Psomas, G. *J. Inorg. Biochem.* **2010**, *104*, 161.
37. Pratviel, G.; Bernadou, J.; Meunier, B. *Adv. Inorg. Chem.* **1998**, *45*, 251.
38. Dimitrakopoulou, A.; Dendrinou-Samara, C.; Pantazaki, A. A.; Alexiou, M.; Nordlander, E.; Kessissoglou, D. P. *J. Inorg. Biochem.* **2008**, *102*, 618.
39. Wilson, W. D.; Ratmeyer, L.; Zhao, M.; Strekowski, L.; Boykin, D. *Biochemistry* **1993**, *32*, 4098.
40. Zhao, G.; Lin, H.; Zhu, S.; Sun, H.; Chen, Y. *J. Inorg. Biochem.* **1998**, *70*, 219.
41. Dhar, S.; Nethaji, M.; Chakravarty, A. R. *J. Inorg. Biochem.* **2005**, *99*, 805.
42. Pasternack, R. F.; Cacca, M.; Keogh, B.; Stephenson, T. A.; Williams, A. P.; Gibbs, F. J. *J. Am. Chem. Soc.* **1991**, *113*, 6835.
43. Novakova, O.; Chen, H.; Vrana, O.; Rodger, A.; Sadler, P. J.; Brabec, V. *Biochemistry* **2003**, *42*, 11544.
44. Psomas, G. *J. Inorg. Biochem.* **2008**, *102*, 1798.
45. Cox, P. J.; Psomas, G.; Bolos, C. A. *Bioorg. Med. Chem.* **2009**, *17*, 6054.
46. Chauhan, M.; Banerjee, K.; Arjmand, F. *Inorg. Chem.* **2007**, *46*, 3072.
47. Hu, Y.; Liu, Y.; Wang, J.; Xiao, X.; Qu, S. *J. Pharm. Biomed. Anal.* **2004**, *36*, 915.
48. Lakowicz, J. R. *Principles of Fluorescence Spectroscopy*, 2nd ed.; Plenum Press: New York, 1999.
49. Wang, Y.; Zhang, H.; Zhang, G.; Tao, W.; Tang, S. *J. Lumin.* **2007**, *126*, 211.
50. Rajendiran, V.; Karthik, R.; Palaniandavar, M.; Stoeckli-Evans, H.; Periasamy, V. S.; Akbarsha, M. A.; Srinag, B. S.; Krishnamurthy, H. *Inorg. Chem.* **2007**, *46*, 8208.
51. Lakowicz, J. R.; Weber, G. *Biochemistry* **1973**, *12*, 4161.
52. Wu, S.; Yuan, W.; Wang, H.; Zhang, Q.; Liu, M.; Yu, K. *J. Inorg. Biochem.* **2008**, *102*, 2026.
53. Marmur, J. *J. Mol. Biol.* **1961**, *3*, 208.
54. Reichmann, M. F.; Rice, S. A.; Thomas, C. A.; Doty, P. *J. Am. Chem. Soc.* **1954**, *76*, 3047.
55. Rigaku/MSC. *CRYSTALCLEAR*, Rigaku/MSC Inc.: The Woodlands, Texas, USA, 2005.
56. Sheldrick, G. M. *SHELXS-97: Structure Solving Program*, University of Göttingen: Germany, 1997.
57. Sheldrick, G. M. *SHELXL-97: Crystal Structure Refinement Program*, University of Göttingen, Germany, 1997.